

A WEAK ALKALI BOND IN (N, K)–A–S–H GELS: EVIDENCE FROM LEACHING AND MODELING

FRANTIŠEK ŠKVÁRA, #VÍT ŠMILAUER*, PETR HLAVÁČEK*, LUBOMÍR KOPECKÝ*, ZUZANA CÍLOVÁ

*ICT Prague, Faculty of Chemical Engineering, Department of Glass and Ceramics,
Technická 5, 16628 Prague 6, Czech Republic*

**Czech Technical University in Prague, Faculty of Civil Engineering, Department of Mechanics,
Thákurova 7, 16629 Prague 6, Czech Republic*

#E-mail: vit.smilauer@fsv.cvut.cz

Submitted August 29, 2012; accepted November 9, 2012

Keywords: Aluminosilicate gel, N–A–S–H gel, Geopolymer, Leaching, Efflorescence

The alkali bond in (N, K)–A–S–H gels presents an up-to-date insufficiently resolved issue with significant consequences for efflorescence in alkali-activated materials. A series of experiments shows nearly all alkalis are leachable from alkali-activated fly-ash and metakaolin in excessive amounts of deionized water. A diffusion-based model describes well the alkali leaching process. Negligible changes of the (N, K)–A–S–H gel nanostructure indicate that Na, K do not form the gel backbone and H_3O^+ is probably the easiest substitution for the leached alkalis. Small changes in the long-term compressive strength of leached specimens support this hypothesis.

INTRODUCTION

The increasing demand for a low-cost and durable construction material stimulates further research in alternative cementitious binders [1 - 5]. Alkali-activated binders based on fly ash or slag represent such a promising group which has stimulated intensive interest worldwide.

The alkali-activation reaction is known from Portland-based materials in which calcium hydroxide promotes the hydrolysis and dissolution of the Si–O group of blended aluminosilicate materials. In contrast to this slow pozzolanic reaction, alkali-activated binders require a much stronger base environment, such as sodium or potassium hydroxides, often exceeding 8M. A detailed analysis of 25 compositions available in open literature revealed that alkali-activated fly ash is normally activated with Na_2O concentrations in the range of 29–237 g/kg of paste with the median 76.6 g/kg, see Fig. 1. These compositions had to meet reasonable workability and the majority of samples experienced curing above 50°C.

Historically, an alkali-activated binder has been called a geopolymer, inorganic polymer, chemically bonded ceramic or alkali-activated cement. Subtle differences originating rather from the commercial background have generated confusion and ill-coordinated research. Furthermore, many of these terms have broadened their meanings over time and started to describe Ca-rich materials as well. For these reasons, the term (N, K)–A–S–H gel is adopted here, describing the

chemical nature of the reaction product rather than its precursor, similar in terminology with C–S–H.

The nanostructure of a poorly crystallized (N, K)–A–S–H gel remains fully unresolved and is still far from being understood. Extensive characterization via NMR, XRD led to the conclusion that the (N, K)–A–S–H gel constitutes a Si–O–Al coordinated 3D network with water filled nanoporosity. Analogous models based on C–S–H or zeolites helped to understand its basic features. Nanoindentation demonstrated intrinsic indentation modulus of the N–A–S–H gel between 17 and 18 GPa on the submicrometers scale, regardless of activated material and curing conditions [6].

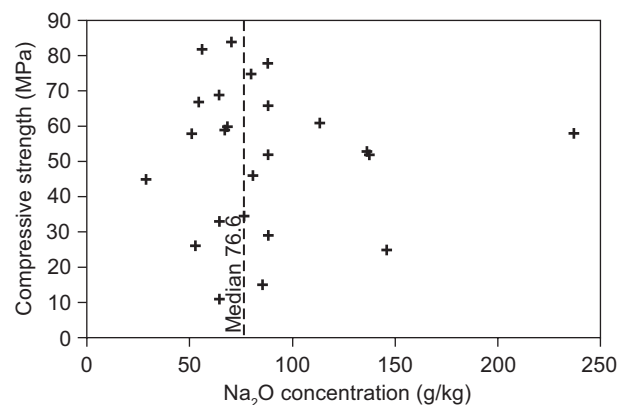


Figure 1. Literature review on Na_2O concentrations in alkali-activated fly-ash from 22 resources (mainly world journals with an impact factor). The SiO_2/Na_2O mass ratio differs in the range between 0 and 1.45.

However, further modeling deduced that basic building blocks of the N–A–S–H gels are different, depending on activating solutions [7].

The role of alkalis in the (N, K)–A–S–H gel seems to draw little attention. Several experiments testified efflorescence problems pointing out to the excessive and weakly bound Na in the gel network [5, 8]. It raises the question whether alkalis are essential elements in the gel nanostructure or they are remnants from the activating solution. This article aims at comparing N, K-leached and unleached (N, K)–A–S–H gels to prove that alkalis can be leached out without affecting the gel skeletal structure, without a loss in strength. This contrasts with C–S–H where calcium leaching leads to a collapse.

Existing models for Na(K) bonds
within (N,K)–A–S–H gels

Glukhovskiy [9] and Krivenko [10, 11] built up models based on the zeolite analogy, primarily related to analcime. They assume the (N, K)–A–S–H gel is amorphous, with randomly distributed little clusters of reciprocal structures, so called short-range-order of SiO₄ tetrahedra and AlO₄ octahedra. A strong Na ionic bond exists within the analcime structure; Na-cations are seated in the centers of the cages of the analcime network. Water molecules fully occupy 16 sites in the unit cell. It is known that Na leaching from zeolites occurs with difficulties, under specific hydrothermal conditions [12], leading to the collapse of zeolite. The model offers no explanation on the weak Na bond and why there is no collapse after the full leaching.

Davidovits [13, 14] formulated a geopolymer model based on the polymeric Si–O–Al network; poly(sialate), poly(sialate-siloxo) and poly(sialate-disiloxo) repetitive units. He described stages in the gel formation, starting with dissolution in a strongly alkaline environment, formation of silanol groups and polycondensation. The weak negative charge on Al^{IV} in the tetrahedral coordination is balanced by Na⁺(K⁺) cations in a strong

ionic binding. Further polycondensation continues into the Na-poly(sialate-disiloxo) albite framework with a feldspar chain structure. The feldspar (albite) crystalline lattice framework is fully reciprocal. Na, (K, Ca) cations are bonded to oxygen in SiO₄ and AlO₄ tetrahedra, but not to alumina, in order to overbalance the excessive negative charge. The leaching of Na (K) alkalis from the feldspar-like structure, without the collapse of the aluminosilicate network of newly formed gel, is in reciprocal contradiction. The leaching of alkalis from the feldspar structure, e.g. during weathering, results in the total collapse of feldspar spatial framework and formation of the sheet silicates and clay minerals.

Fernández-Jiménez et al. [15] presented a model inspired by the sol-gel process. The colloids themselves form cross-links leading to 3-D structures. The Al₂O₃/K₂O ratio equals one since certain other ions must be included in the structure to offset the electrical imbalance generated when Al³⁺ ions replace Si³⁺ ions in the polymer. The Al in these gels is tetrahedrally coordinated.

Cloos et al. [16] assume that silico-alumina gels are based on Si⁴⁺, occurring in a tetrahedral coordination with a partial substitution of Al⁴⁺ (Al³⁺). The negative charge in the core is compensated by the positive charge of mono- or polymeric hydroxyaluminium cations Al(OH)₂⁺. Increasing the Al/(Al+Si) ratio, the complexity of these polymeric cations increases, whilst the net charge per alumina atom decreases. At very high Al/(Al+Si) ratios (> 0.8), this charge tends to zero and a demixing is observed and the next phases (pseudo-boehmite and bayerite) appear.

Mason et al. [17] assume that the existence of Al^{IV} in association with Si^{IV} requires an additional charge and structural balancing components in the form of Na⁺ (K⁺) cations. The spectra of 9.4 T ²³Na NMR reveal that the positions of the peaks are similar to those observed for sorpted Na⁺ on the surface of silica. The hydration state suggests the Al^{IV} phase is kaolinite-like, and the ²⁹Si data indicates that at least in one case allophane is present.

Barbosa et al. [18] consider the gel as randomly

Table 1. Basic models N(K)–A–S–H gels and Na(K) bond.

Authors	Analogy	Na(K) bond within N(K)–A–S–H gels
Glukhovskiy [9], Krivenko [10,11]	Zeolites, analcime	Alkali cations are linked with a strong ionic bond within the Si–O–Al network and remain hardly leachable.
Davidovits [13,14]	Organic polymer	Na ⁺ (K ⁺) compensate a weak negative charge on Al ^{IV} . Further polycondensation into the Na-poly(sialate-disiloxo) albite framework with a feldspar chain structure.
Fernández-Jiménez et al. [15]	Synthetic gel, colloid	Na ⁺ (K ⁺) compensate a weak negative charge on Al ^{IV} .
Cloos et al. [16]	Synthetic gel, colloid	Al(OH) ₂ ⁺ or Al _n (OH) _m ^{(3n-m)+} compensate a charge of Al ⁴⁺ in the tetrahedral coordination. The Na ⁺ bond remains unaddressed.
Mason et al. [17]	Synthetic gel	Na ⁺ (K ⁺) compensate a weak negative charge on Al ^{IV} .
Barbosa et al. [18]	Organic polymer	Na(H ₂ O) _n ⁺ , K(H ₂ O) _n ⁺ compensate a weak negative charge on Al ^{IV} .

oriented Al, Si polymeric chains providing cavities of sufficient size to accommodate the charge-balancing hydrated Na ions in the form of $\text{Na}(\text{H}_2\text{O})_n^+$, $\text{K}(\text{H}_2\text{O})_n^+$. The model allows easy cation leaching while keeping a positive-negative charge balance.

EXPERIMENTAL

Materials and methods

Fly ash of class F originated from the Opatovice brown-coal power plant, Czech Republic. Metakaolin from the Sedlec location, Czech Republic, was prepared from ordinary kaolin treated at 750°C for 24 hours. Table 2 provides chemical compositions of both materials.

Table 3 provides initial compositions for Na, K alkali-activated fly ash and metakaolin which are denoted further as AAFA and AAMK. The compositions were optimized to meet standard workability and possess compressive strength above 40 MPa. Sodium and potassium metasilicate solutions were intermixed with NaOH or KOH and water added. All samples were cured at 80°C for 12 hours and stored in a 20–25°C environment under RH 45–50 %, if not specified differently.

Experimental methods included XRD (PANalytical X'Pert PRO Philips), FTIR (Nicolet 740 Nexus), NMR MAS (^{29}Si , ^{27}Al , ^{23}Na , BrukerAvance 500WB/US), EDX+ EBSD (XL 30 ESEM), AAS (Varian Spectr AA880). More detailed study was devoted to raw fly ash

using electron microscopy (Hitachi S-4700 coupled with the SDD detector) with analyzer XRF (ARL 9400/HP+). Particular details of leaching conditions and specimens' geometries are provided in the following subsections.

RESULTS AND DISCUSSION

Before proceeding to leaching experiments, alkali leachability from inactivated materials had to be assessed. Raw fly ash contains certain amounts of Na, K, see Table 2. Immersing 20 g of raw FA into 1000 g of deionized water and constant shaking for 72 hours revealed that only 1.7 % of Na_2O and 0.8 % of K_2O had leached out. For this reason, the alkalis present in FA and MK were neglected in the assessment of the overall leaching balance.

Remaining Na, K in (N, K)–A–S–H gels after long-term leaching

A sufficiently long Na, K leaching from AAFA and AAMK reveals an asymptotic concentration of alkalis in (N, K)–A–S–H gels. To speed up the leaching process, paste samples were crushed under the size of 0.5 mm and leached 150 days in deionized water with regular water exchange between 1 and 3 days. The content of Na, K was determined using X-ray fluorescence analysis. Table 4 shows the initial and final concentrations of Na_2O and K_2O in the geopolymer paste; only 2 % of Na_2O and

Table 2. Chemical compositions of fly ash and metakaolin.

Oxide (wt. %)	SiO_2	Al_2O_3	Na_2O	K_2O	CaO	MgO	Fe_2O_3	TiO_2
Fly ash	53.52	32.87	0.33	2.05	1.80	0.85	5.89	1.89
Metakaolin	50.43	46.20	0.03	1.07	0.38	0.27	1.07	0.27

Table 3. Initial compositions of pastes and mortars in terms of mass ratios.

	$\text{SiO}_2/(\text{Na,K})_2\text{O}$	$\text{H}_2\text{O}/(\text{Na,K})_2\text{O}$	Activator/(FA, MK)	Fly ash/sand	Initial $(\text{Na,K})_2\text{O}/\text{all}$ [g/kg]
Paste, fly ash, Na	1.06	4.57	0.46	–	47.81
Paste, fly ash, K	1	3.14	0.36	–	51.47
Paste, metakaolin, Na	1	3.5	1.1	–	95.24
Paste, metakaolin, K	1	3.5	1.1	–	95.24
Mortar, fly ash, Na	1.06	4.28	0.44	1:1.5	23.78
Mortar, fly ash, K	1	3.85	0.41	1:1.5	24.05

Table 4. Concentration of M_2O in the geopolymer before and after leaching for 150 days.

	Initial concentration $\text{M}_2\text{O}/\text{initial mass}$ [g/kg]	Final concentration after 150 days of leaching $\text{M}_2\text{O}/\text{initial mass}$ [g/kg]	Molar concentration M^+/Al^- in N–A–S–H gel before leaching [mol/mol]	Molar concentration M^+/Al^- in N–A–S–H after leaching [mol/mol]
AAFA, Na	47.81	0.96	0.7	0.01
AAFA, K	51.47	0.77	0.46	0.01
AAMK, Na	95.24	5.71	0.72	0.04
AAMK, K	95.24	1.9	0.47	0.01

1.5 % of K_2O remained in AAFA and 6 % of Na_2O and 2 % of K_2O in AAMK. This shows that Na, K are weakly bound in the (N, K)-A-S-H gel and could be almost completely leached out.

The theoretical molar ratio M^+/Al^- is calculated from the amount of dissolved Al from fly ash or metakaolin which combined to the (N, K)-A-S-H gel. The Al leaching from hardened AAFA after 18 days was found to be only 0.1 % of the overall Al amount, therefore leached Al can be neglected. The degree of reaction for AAFA was previously estimated as 0.5 and for AAMK as 0.99 [6]. Table 4 provides molar ratio M^+/Al^- before and after leaching. Considering the charge-balancing interaction between (Na^+, K^+) and Al^- , the leached alkali cations need to be replaced. We hypothesize H_3O^+ presents the most suitable replicant.

Leaching kinetics of Na_2O from N-A-S-H gels and modeling

The previous section proved almost full leaching of Na, K from the AAFA and AAMK pastes. The following experiment quantifies the Na leaching kinetics from AAFA. A sodium-activated AAFA specimen with the size of $40 \times 40 \times 160$ mm was submerged into 600 ml of deionized water, where the water had regular replacement between one and three days. The concentration of Na in the water bath was measured after each water replacement.

Table 5 summarizes the measured concentrations of Na_2O during 18 days. The remaining Na_2O in the paste was deduced from the leached Na and the initial concentration, see Table 3.

The unknown diffusion coefficient for the Na transport was determined using the 3D leaching simulation in the OOFEM software [18]. One eighth of the $40 \times 40 \times 160$ mm sample was considered due to symmetry reasons, see Figure 2 for the geometry. The numerical

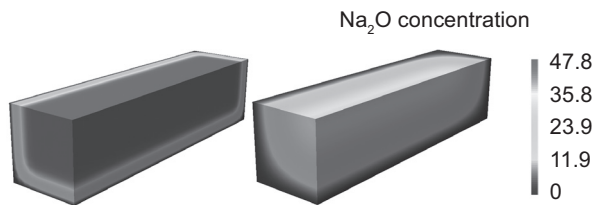


Figure 2. Na leaching simulation on an eighth of the $40 \text{ mm} \times 40 \text{ mm} \times 160 \text{ mm}$ prism. Concentrations of Na_2O (g/kg) in the AAFA paste after 28 days of leaching (left) and after 365 days of leaching (right).

simulation assumes the diffusion coefficient to be constant and independent of the concentration. It is well known that the water vapor diffusivity coefficient drops by a factor of approximately 20 for mature concrete [20]. Nonlinear diffusion would cause a slowdown in the leaching process. However, the asymptotic values are retained. Figure 3 shows the average concentration of Na_2O in the paste during the leaching experiment and the results from the numerical simulation. The diffusion coefficient for the Na transport in the AAFA was fitted to $D = 1.6 \cdot 10^{-7} \text{ m}^2/\text{day}$. Figure 2 depicts the concentration field at 28 days and 365 days of leaching.

Na_2O profile from EDX analysis

The Na_2O concentration profile from the sample surface could be verified independently by EDX analysis. Surface areas were cut from the 28 day-leached AAFA and AAMK prisms and exposed to an EDX line analysis. Figure 4 shows the Na_2O concentration profile with strongly heterogeneous values. Analytical solution of a linear diffusion equation leads to the error function [20]

$$c(x, t) = c_{init} \operatorname{erf}\left(\frac{x}{2\sqrt{Dt}}\right) \quad (1)$$

where c_{init} is the initial concentration of Na_2O in the body, $c(x, t)$ is the concentration at a given time and the position x from the surface, D represents the constant diffusion coefficient and the time t represents 28 days.

Figure 4 displays analytical solution for AAFA and AAMK with measured data. The upper and lower feasible bounds are displayed with corresponding diffusion coefficients. Due to higher porosity of AAMK, the diffusion coefficient attains a higher value. Note that the

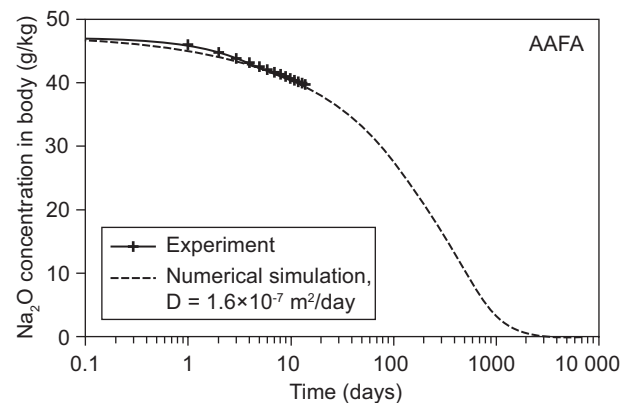


Figure 3. Concentrations of Na_2O in the AAFA paste. The prism $40 \times 40 \times 160$ mm was leached in deionized water which was regularly replaced.

Table 5. Concentration of Na_2O in the water bath during the leaching experiment.

Time [day]	1	2	3	4	7	8	9	10	11	14	15	16	17	18
Conc. [g/l]	3.96	2.66	2.02	1.53	2.95	1.12	0.86	0.78	0.72	1.33	0.61	0.52	0.48	0.43

measured concentration profiles reach non-zero values on the surface since certain transport occurs during the preparation for EDX analysis.

Visible evidence for efflorescence

Exposing Na-activated materials to a moisture-gradient environment leads to the formation of efflorescence [5], Figure 5. The leaching of Na from the bulk activated material reacts with atmospheric CO₂ and forms visible carbonates, hydrocarbonates and sulfates. The analysis of efflorescence products revealed no crystalline silicates.

Alkali transport could be mitigated when samples are exposed to RH < 30 %. Such low humidity seems to be sufficient for breaking-up continuous pore channels for ion transport. Any rewetting of a sample surface reactivates the transport mechanisms and efflorescence

reappears after a short time.

Exposing wet polished samples to a low vacuum environment leads to a quick formation of efflorescence. Figure 6 shows the beginning stage of surface efflorescence on AAFA.

SEM of leached samples and compressive strength

No visible changes on fracture surfaces were observed in leached AAFA specimens for 3 years, Figure 7. The samples were immersed in a sealed container with deionized water which was exchanged every week. No observable differences are evident for AAMK leached for 3 months, Figure 8.

No degradation of N–A–S–H gels after leaching

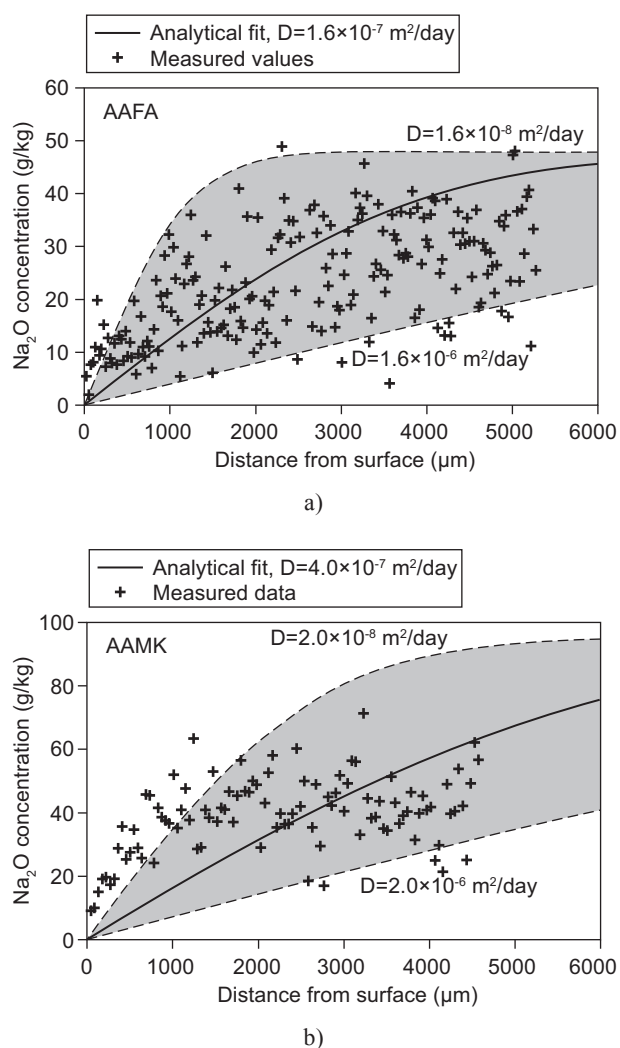


Figure 4. The Na₂O concentration profile in AAFA (a) and AAMK (b) after 28 days of leaching in deionized water. Measured points in black were gathered using the EDX linear analysis. Black lines show solution via error function with feasible lower and upper bounds.

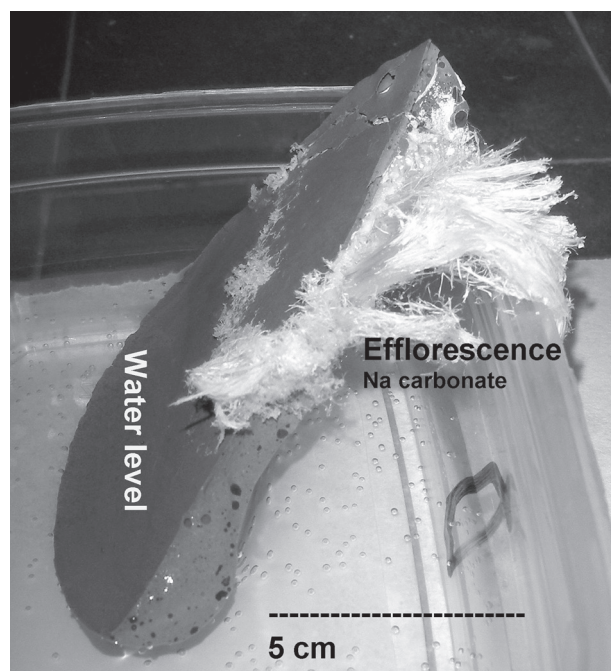


Figure 5. High efflorescence after 50 days of partially-immersed AAFA.

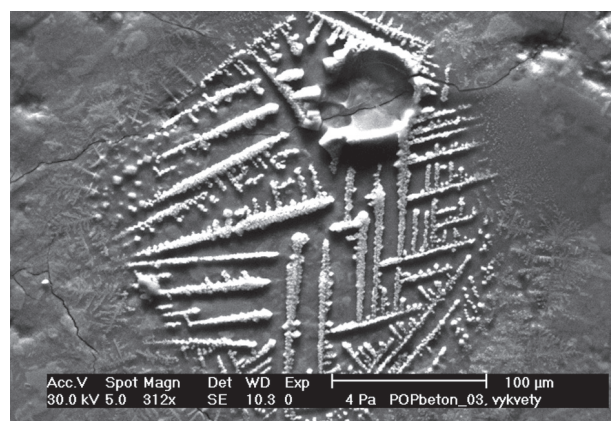


Figure 6. Efflorescence on the surface of AAFA (Na₂CO₃, NaHCO₃) in ESEM.

is supported via compressive strength measurement on AAFA mortars, Figure 9. The specimens (4×4×16 cm) were left for 550 days on air or immersed in water. Different strengths within air and water-cured samples could be partially attributed to the fact that dry concrete exhibits higher strength due to higher cohesion forces between the gel particles.

When a strength decrease is associated with the process of Na leaching, gradual strength degradation would occur, which is not the case here. Similar findings were observed on samples immersed up to two years in water [21-24]. This indicates only the Si-O-Al-O-Si chain forms a load-bearing nanostructure within the N-A-S-H gel and Na is bound weakly, practically unaffacting compressive strength.

This strongly contrasts with C-S-H-based materials, where calcium leaching of Portland pastes in the ammonium nitrate solution proved a significant reduction in compressive strength to about one fourth of sound samples [25, 26]. The nanoindentation experiment

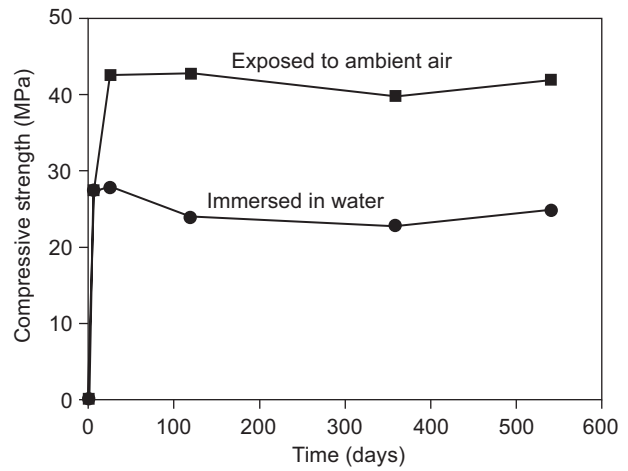
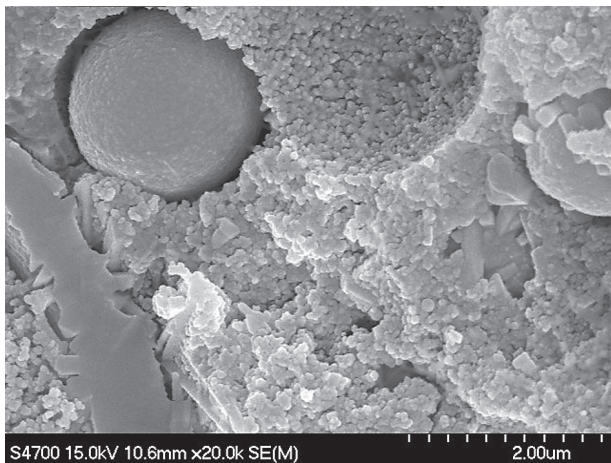


Figure 9. Compressive strength evolution of AAFA mortars. The samples were exposed to ambient air or immersed in water at 20-25°C.



a)



b)

Figure 7. AAFA samples unleached (left) and leached for 3 years (right), fracture surface in SEM.



a)



b)

Figure 8. AAMK samples unleached (left) and leached for 3 months (right), fracture surface in SEM.

testified that the elastic modulus of low-density type C–S–H dropped from 21.7 to 3.0 and that of C–S–H high-density type dropped from 29.4 to 12 GPa [27]. These findings clearly demonstrate Ca being a significant part of the C–S–H gel while Na being abundant in the N–A–S–H gel.

^{29}Si , ^{27}Al NMR MAS spectra of Na-activated AAFA and AAMK

The ^{29}Si and ^{27}Al NMR spectra of leached and unleached AAFA samples are essentially the same, without any noticeable changes exceeding the NMR inaccuracies. Leached samples were 150 days in deionized water with regular water exchange between 1 and 3 days.

The ^{29}Si spectra for AAMK show a small difference which is probably attributed to the peak at -109.3 ppm, previously ascribed to crystalline silica phases [3]. Both AAFA and AAMK indicate that the Si–O–Al backbone remains essentially the same before and after Na leaching.

Mitigation of Na leaching and ^{23}Na MAS NMR

Na leaching drops to almost zero when AAFA samples are exposed to temperatures over about 600°C for 2 hours. Figure 12 demonstrates the Na_2O concentration in the water bath (1:50 by mass) after the 24 hour exposure of prismatic samples 40×40×160 mm. The change indicates that Na enters directly into the structure of the N–A–S–H gel and becomes an integral part of the newly formed sodium silicate glass as demonstrated in the following ^{23}Na NMR MAS spectra.

The ^{23}Na NMR MAS spectra in Figure 13 show that at 20°C Na occurs in the structure in the form of $\text{Na}(\text{H}_2\text{O})_n^+$ where $n = 2-8$ [28]. The peak at -4 ppm is attributed to the sodium associated with Al inside the gel nanostructure [3]. The shift to negative values above 400°C is attributed to water evaporation. A further series of peaks in the spectrum at 400–600°C corresponds to the overall rearrangement of the N–A–S–H gel structure. A dominant peak at -14ppm occurs at 600°C, which corresponds to the structure of sodium silicate glass

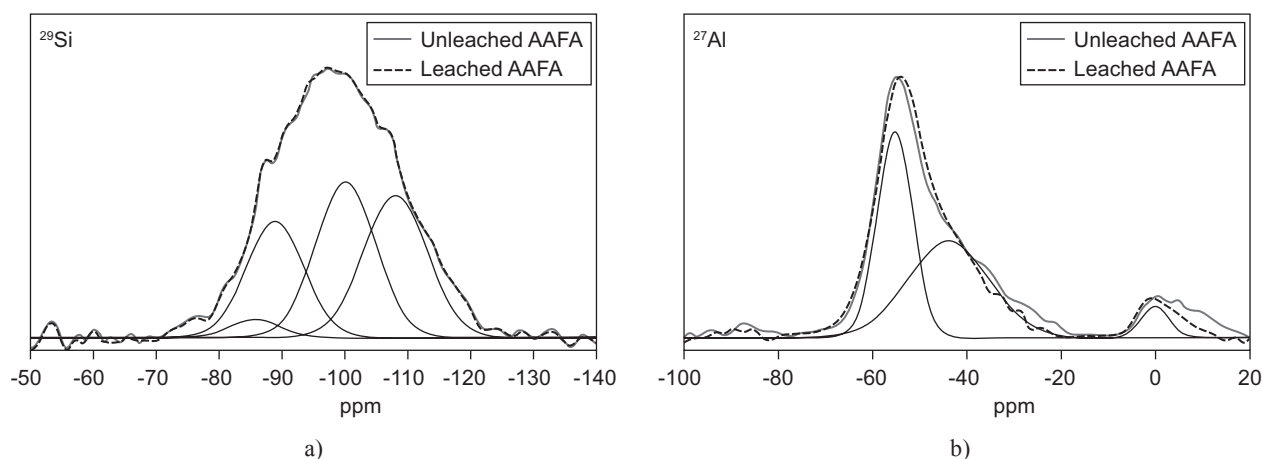


Figure 10. ^{29}Si and ^{27}Al NMR MAS spectra for AAFA. Deconvolution spectra plotted for unleached samples.

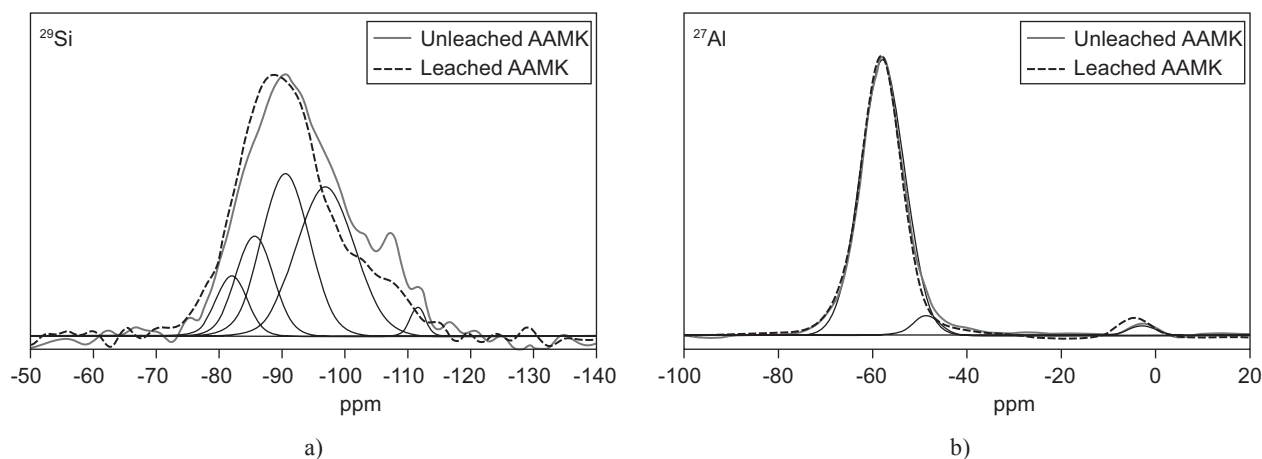


Figure 11. ^{29}Si and ^{27}Al NMR MAS spectra for AAMK. Deconvolution spectra plotted for unleached samples.

[29, 30]. The ^{39}K NMR spectrum demonstrated a similar effect [30]. Therefore, Na acts as a melting agent above 600°C and becomes embedded within sodium silicate glass.

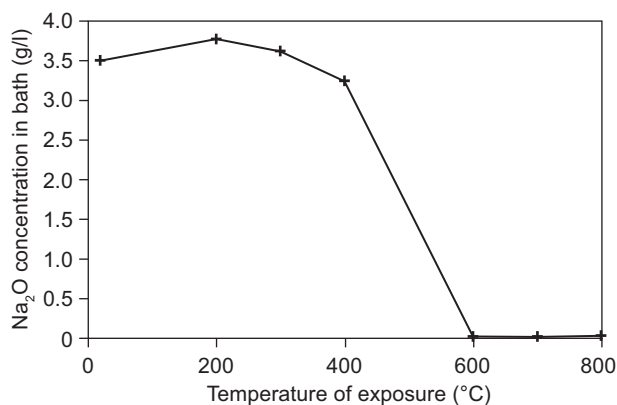


Figure 12. Na leachability from the AAFA paste in dependence on the previous temperature history.

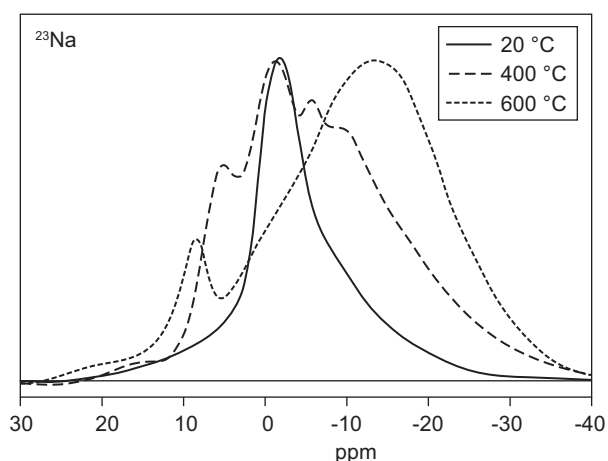


Figure 13. ^{23}Na NMR MAS spectra of AAFA in dependence on the thermal history.

Refined model for the alkali bond within (N,K)-A-S-H gels

A weak Na, K bond in (N, K)-A-S-H gels could be interpreted using the model from Barbosa et al. [18]. The positively-charged alkali cation can be replaced with other cations present in the system, see Figure 14. The most probable is H_3O^+ but $\text{Al}(\text{OH})_2^+$ or $\text{Al}_n(\text{OH})_m^{(3n-m)+}$ could also compensate the negative charge according to Cloos et al. [16]. The presence of other metal cations (Fe, Mn, Ca, K) in the geopolymer precursor (metakaolin, fly ash) can also easily balance the negative charge on Al^{IV} . The refinement for the alkali bond presents a minor adjustment in the 3D model of the Si-O-Al-O-Si network.

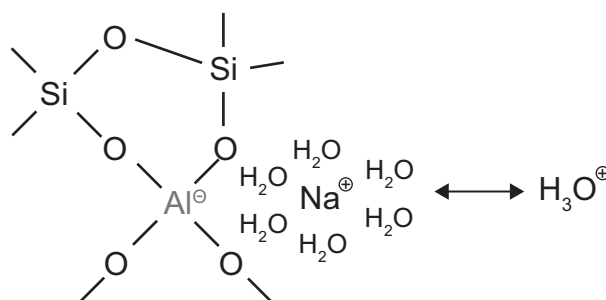


Figure 14. An alkali bond according to Barbosa et al. [18] and its replacement with an H_3O^+ cation during leaching.

CONCLUSIONS

The series of experiments demonstrated a weak bond of Na(K) in the (N, K)-A-S-H gel. The analyses of the Na, K role in alkali activated fly ash and metakaolin-based systems lead to the following conclusions:

1. Na, K create a strong base environment for the dissolution of glass phases from activated materials in accordance with up-to-date knowledge. Na, K is bound only weakly in the nanostructure of the (N,K)-A-S-H gel and is leachable almost completely. This causes alkali-activated materials to be prone to efflorescence with excessive remnants of alkalis in the system. (Na,K)OH easily diffuses to the surface where it reacts with atmospheric CO_2 while forming visible salts such as $\text{Na}_2\text{CO}_3 \cdot n\text{H}_2\text{O}$, NaHCO_3 , K_2CO_3 , KHCO_3 .
2. Almost all Na can be leached out from the gel without compromising compressive strength. This renders Na as an unnecessary load-bearing element in the nanostructure of the N-A-S-H gel and demonstrates A-S-H to be a load-bearing structure. In such particular case, the Al negative charge must be balanced by another cation, probably by readily available H_3O^+ .
3. The diffusivity for Na leaching was found between $1.6 \cdot 10^{-7}$ and $4.0 \cdot 10^{-7}$ m^2/day . Similar values are expected for K.
4. Exposing Na-activated fly ash to temperatures over 600°C practically stops Na leaching. This is explained by Na embedding inside the newly formed glasses.

Acknowledgement

We gratefully acknowledge the financial support from the Czech Science Foundation GAČR under projects P104/12/0102 and P104/10/2344.

References

1. Gartner E.M., Macphee D.E.: *Cem. Concr. Res.* 47, 736 (2011).
2. Pacheco-Torgal F., Castro-Gomes J., Jalali S.: *Constr. and Build. Mater.* 22, 1305 (2008).
3. Provis J.L., van Deventer J.S.J. et al.: *Geopolymers, structure, processing, properties and industrial applications*, CRC Press 2009.
4. Škvára F., Kopecký L., Šmilauer V., Bittnar Z.: *J. Hazard. Mater.* 168, 711 (2009).
5. Škvára F., Kopecký L., Myšková L., Šmilauer V., Albeirovská L., Vinšová L.: *Ceramics-Silikáty* 53, 276 (2009).
6. Němeček J., Šmilauer V., Kopecký L.: *Cem. Concr. Comp.* 33, 163 (2011).
7. Šmilauer V., Hlaváček P., Škvára F., Šulc R., Kopecký L., Němeček J.: *J. Mater.Sci.* 46, 6545 (2011).
8. Ly L., Vance E.R., Perera D.S., Aly Z., Olufson K.: *Adv. in Tech. of Mat. and Mat. Proc. J.* 8, 239 (2006).
9. Glukhovskiy, V.D.: *Soil Silicates* (Gruntosilikaty), Budivelnik Publish, Kiev, Ukraine 1967.
10. Krivenko P.: *Adv. in Sci. and Tech.* 69, 1 (2010).
11. Krivenko P., Kovalchuk G.: *J. Mater. Sci.* 42, 2944 (2007).
12. Klika Z., Weiss Z., Mellini M.: *Acta Geodynamica et Geomaterialia* 2, 1 (2005).
13. Davidovits J. in: *Proc. 2nd Inter. Conf. Géopolymère 1999*, p. 9-40, Ed. J. and R. Davidovits, C. James, Institut Géopolymère 1999.
14. Davidovits J.: *Geopolymers Chemistry and Applications*, 2nd ed. Institut Géopolymère 2008.
15. Fernández-Jiménez A., Vallepu R., Terai T., Palomo A., Ikeda K., *J. Non-Cryst. Solids* 352, 2061 (2006).
16. Cloos P., Léonard A.J., Moreau J.P., Herbillon A., Fripiat J.J.: *Clays Clay Miner.* 17, 279 (1969).
17. Mason H.E., Maxwell R.S., Carroll S.A.: *Geochim. Cosmochim. Acta* 75, 6080 (2011).
18. Patzák B., Bittnar Z.: *Advances in Eng. Soft.*, 32, 759 (2001).
19. Barbosa V.F.F., Mac Kenzie K.J.D., Thaumaturgo C.: *Intern. J. Inorg. Mater.* 2, 309 (2000).
20. Vedalakshmi R., Saraswathy V., Song H.W., Palaniswamy N.: *Corros. Sci.* 51, 1299 (2009).
21. Hardjito D., Rangan B.V.: *Research Report GC 1*, Curtin University of Technology, Perth, Australia 2005.
22. Hardjito D., Wallah S.E., Sumajouw D.M.J., Rangan B.V.: *ACI Mater. J.* 101, 67 (2004).
23. Wallah S.E., Hardjito D., Sumajouw D.M.J., Rangan B.V. in: *Proc. ICFRC Inter. Conf.*, p. 527 – 539, Ed. Parameswaran V.S., Pub. Allied Publishers Private Limited, New Delhi 2004.
24. Strnad T., PhD Thesis, Czech Technical University in Prague, 2010.
25. Kamali S., Moranville M., Leclercq S.: *Cem. Concr. Res.* 38, 575 (2008).
26. Carde C., Raul F.: *Cem. Concr. Res.* 27, 539 (1997).
27. Constantinides G., Ulm F.J.: *Cem. Concr. Res.* 34, 67 (2004).
28. Maekawa H., Saito T., Yokokawa T.: *J. Phys. Chem. B* 102, 7523 (1998).
29. Tossell J.A., *Phys. Chem. Minerals* 27, 70 (1999).
30. Phair J.W., van Deventer J.S.J.: *Minerals Eng.* 14, 289 (2001).